

An experimental study on tailings deposition characteristics and variation of tailings dam saturation line

Guangjin Wang^{1a}, Sen Tian^{*2}, Bin Hu^{**3}, Xiangyun Kong¹ and Jie Chen^{2b}

¹Engineering Research Center for Green Comprehensive Utilization of Metal Ore Tailings Resources, Faculty of Land Resources Engineering, Kunming University of Science and Technology, Kunming 650093, China

²State Key Laboratory of Coal Mine Disaster Dynamics and Control, School of Resources and Safety Engineering, Chongqing University, Chongqing 400044, China

³Hubei Key Laboratory for Efficient Utilization and Agglomeration of Metallurgic Mineral Resources, School of Resources and Environmental Engineering, Wuhan University of Science and Technology, Wuhan 430081, China

(Received March 16, 2020, Revised August 3, 2020, Accepted September 10, 2020)

Abstract. This study adopted soil test and laboratory physical model experiments to simulate the tailings impoundment accumulation process according to the principle of similarity. Relying on the practical engineering, it analyzed the tailings deposition characteristics on dry beach surface during the damming process, as well as the variation rules of dam saturation line. Results suggested that, the tailings particles gradually became finer along the dry beach surface to inside the impoundment. The particle size suddenly changed at the junction between the deposited beach and the water surface, which displayed an obvious coarsening phenomenon. Besides, the deposited beach exhibited the vertical feature of coarse upward and fine downward on the whole. Additionally, in the physical model, the saturation line elevated with the increase in dam height, and its amplitude was relatively obvious within the range of 1.0-4.5 m away from the initial dam. Under flood condition, the saturation line height was higher than that under normal condition on the whole, with the maximum height difference of 4 cm. This study could provide an important theoretical basis for further studies on dam failure experiments and the evolution rules of leaked tailings flow.

Keywords: geotechnical slope; taings dam stability; deposition characteristics; saturation line; physical model

1. Introduction

With the rapid development of current mining industry in recent years, the number and scale of tailings impoundment are increasing (Tian and Chen 2015). Tailings impoundments are the essential structure during the normal production of mine, which are also the potential major hazard source in the safe production of mine (Yin *et al.* 2011, Wang *et al.* 2019, Santamarina *et al.* 2019). In case of tailings dam failure, the tailings, mud and water in the impoundment are discharged downward to form the mudslide, which severely damage the life and property of the downstream residents, and induce serious environmental disaster (Darren *et al.* 2019, Nam *et al.* 2019, Rico *et al.* 2008). The cause and mechanism of dam break vary to some extent among different tailings impoundments (Zheng *et al.* 2019, Zhou and Cheng 2014). Currently, various theoretical analyses and experimental measurements are performed to explore the mechanism of tailings dam failure.

It has been found that, main external causes of dam failure include seepage failure, dam foundation instability, flood overtopping, and earthquake-induced liquefaction (Zhang *et al.* 2019, Tian *et al.* 2017, Sun *et al.* 2012).

With regard to the stability of tailings impoundment, on the one hand, it is determined by the tailings physical-mechanical properties and the stockpiling pattern (Jing *et al.* 2019); on the other hand, it is determined by the tailings particle deposition characteristics (Parbhakar-Fox *et al.* 2018, Wang *et al.* 2018, Jia *et al.* 2012). Therefore, it is of great significance to investigate the deposition rules of dry beach particles in tailings impoundment for evaluating the tailings impoundment stability; meanwhile, it is of guiding significance to optimize the ore drawing manner in the mine (Muceku *et al.* 2016, Wei *et al.* 2013). At present, the upstream damming method is extensively adopted in tailings impoundment, in which the deposition rules of dry beach particles are affected by factors like tailings particle size, pulp density, flow velocity, ore drawing location and ore drawing method. As a result, the deposition characteristics of tailings particles on the dry beach surface are extremely complicated, which also lead to obvious differences in tailings particle composition and physical-mechanical properties (Dutto *et al.* 2017, Cai *et al.* 2019, Marsooli and Wu 2014). While saturation line is the direct manifestation of tailings dam safety, which is the intersection between the seepage flow surface and the dam body cross section. Its downside soil mass is at a saturated status; due to the seepage force of seepage water, the

*Corresponding author, Ph.D.

E-mail: sentian@cqu.edu.cn

**Corresponding author, Professor

E-mail: hbin74@wust.edu.cn

^aProfessor, Ph.D.

E-mail: wanguangjin2005@163.com

^bProfessor, Ph.D.

E-mail: jiechen023@cqu.edu.cn



Fig. 1 The components and structures of tailings impoundment

position and shape of saturation line inside the dam body have great impacts on the dam body stress, soil mass shear strength and dam body permeability stability.

Currently, researchers have carried out extensive investigations on dam break mechanism and dam break simulation (Deng *et al.* 2016, Alhasan *et al.* 2016). However, little research is done on the tailings particle deposition rules based on the laboratory damming physical model experiments and field experiment, and more indepth and systemic research is necessary (Owen *et al.* 2020, Mizani 2010). By using physical model experimental investigation, the prototypical mechanics and motion were deduced according to principle of mechanical similarity. It helped to more intuitively reflect the engineering practice, more precisely predict the prototype stability development trend, and probe the dam body defect.

Therefore this study adopted the real tailings impoundment as the prototype, the tailings from the dry beach surface and dam body were sampled for screening experiments. Besides, the soil test and laboratory physical model experiments were performed to simulate the tailings damming process according to the principle of similarity. It then analyzed the tailings deposition characteristics on dry beach surface during the damming process, and the variation rules of dam saturation line, relying on the practical engineering. The experimental results were consistent with the practical engineering and numerical

simulation results of this research (Li *et al.* 2020, Wang *et al.* 2019). This study could provide an important theoretical basis for further studies on tailings dam stability, and the evolution simulation of leaked tailings flow.

2. Model and computational method

In this study, a tailings impoundment in Sichuan Province of China was treated as the engineering background. This tailings impoundment is the valley-type tailings impoundment, with the geomorphic unit of mountain alternating with ravine landform. In that tailings impoundment, the dam was constructed at the valley mouth, the width at the dam axis was about 120 m, which was gradually widened towards the interior of valley, and the maximum width of effective tailings accumulation range reached about 1200 m at the valley bottom. The terrains in both sides of hillsides were slow, which changed by about 25°-35° along with the landform, and the total catchment area inside the impoundment was about 6.51 km².

2.1 Geological conditions of tailings impoundment

The initial dam crest elevation in that tailings impoundment was 1975 m, the dam height was 32.0 m, the designed dam surface width was 4.0 m, the downstream

Table 1 Tailings particles size distribution parameter

Tailings Type	Size Distribution/ %						d_{10}	d_{30}	d_{50}	d_{60}	Cu	Cc
	<0.074	<0.1	<0.25	<0.5	<1	<2						
Medium sand	14.50	24.24	46.33	79.34	96.32	99.22	0.040	0.139	0.278	0.354	8.850	1.364
Fine sand	14.08	27.51	66.43	92.37	98.19	99.52	0.042	0.110	0.187	0.225	5.357	1.280
Silt	43.34	62.35	94.80	99.81	99.99	100.00	0.006	0.036	0.097	0.083	15.397	2.121

Table 2 Tailings basic physical and mechanical parameters

Tailings sample	Moisture content ω / %	Osmotic coefficient	Void ratio /e	Proportion Gs	Cohesive force c/ kPa	Internal friction angle ϕ / °
Medium sand	19.00	7.44×10^{-3}	0.55	2.70	55.42	31.70
Fine Sand	9.90	5.76×10^{-3}	0.85	2.92	49.18	31.85
Silt	19.00	5.19×10^{-3}	0.55	2.70	40.15	31.31
Based soil	20.00	4.36×10^{-7}	0.46	1.80	21.17	31.95

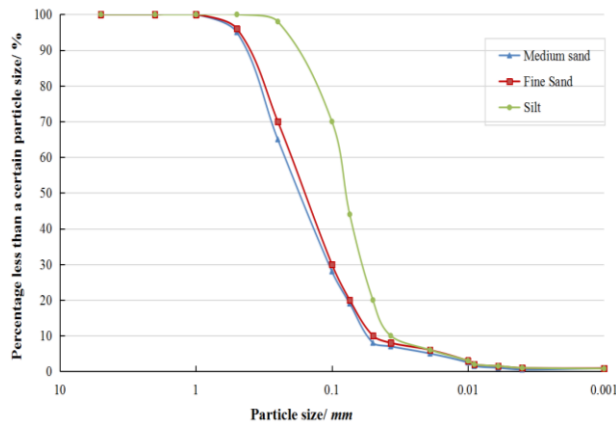


Fig. 2 Tailings particles grading curves

dam slope ratios were 1:2 and 1:5, while the upstream dam slope ratio was 1:1.75. Besides, the external bottom width of the initial dam was 13.98 m, the internal bottom width was 12.7 m, the top width was 131.8 m, the dam body bottom thickness at vertical dam axis direction was 161.8 m, the dam height was 36.0 m, and the overall dam volume was about 139600 m³.

The fill dam crest elevation in that tailings impoundment was 2005 m (the height above sea level), and the dam height was 62 m. The upstream damming technology was adopted, the subdam was constructed using the coarse particle tailings deposited in front of the impoundment, each level of subdam was 5 m in height, with the external slope ratio of 1:3.5, and the total slope ratio of 1:4.233. The sub-dams located upstream of the main dam, where the tailings can be deposited and, consequently, the decrease of the streambed slope and the increase of the storage capacity of the reservoirs.

The dry beach length of the tailings impoundment was always over 350 m, and the average slope ratio of the dry beach was 1.55%. Facilities, such as impervious dam (pond), pump station and backwater dam, were set in the downstream reservoir area, and the capacity of reservoir was about 300000 m³. The components and structures of tailings impoundment are displayed in Fig. 1.

2.2 Tailings physical-mechanical parameters

Field sampling was carried out for soil mechanical tests, such as particle screening, permeability tests, and triaxial shear test, so as to examine the tailings particles size distribution and physical-mechanical properties (Aly *et al.* 2012, Gawu and Fourie 2004, Pashias 1996), as presented in Table 1 and Table 2. Meanwhile, the tailings particle grading curve was obtained, as exhibited in Fig. 2.

where, d_n denotes the mass percentage (n%) of particles smaller than such particle size in the total particle mass; Cu and Cc represent uniformity coefficient and coefficient of curvature, respectively. Additionally, medium sand suggested that the mass of particles with the particle size >0.25 mm accounted for 50% of the total mass. Fine sand represents that mass of particles with the particle size >0.074 mm accounted for 85% of the total mass, while that of silt accounted for 50%.

In Table 1 and Fig. 2, the tailings contents within the three particle size ranges differed substantially, which might be mainly induced by the inter-particle acting force. A large number of small particles were adhered onto the large particles, and the crude and fine particles might not be completely separated when selecting, thus increasing the content of large particles. The grading uniformity coefficients of samples (Cu) were greater than 5, and the coefficients of curvature (Cc) were between 1 and 3, which displayed unevenness and well grading of the samples.

In Table 2, the tailings basic physical and mechanical properties provided basic parameters for the physical model experiments. They mainly included moisture content, void ratio, proportion, cohesive force, shear strength, etc. Meanwhile, they offered the fundamental data for analyzing the tailings dam stability.

2.3 Similar physics parameters

According to the tailings impoundment design data and reservoir area landform, the geometric proportion of this experiment was determined to be 1:150, in other words, $\lambda_l = l_p/l_m = 150$. According to the Froude similarity



(a) Dry beach surface formed during the damming process



(b) Full view of the physical model after damming

Fig. 3 The experimental site of the physical model

Table 3 Similarity scale between model and prototype parameters

Parameters	Ratio Scale	Parameters	Ratio Scale
Length	$\lambda_1=150$	Rate of flow	$\lambda_Q=\lambda_1^{2.5}=150^{2.5}$
Displacement	1:150	Volume	1:150 ³
Flow velocity	$\lambda_v=\sqrt{\lambda_1}=150^{0.5}$	Cut-off area	$\lambda_A=\lambda_1^2=150^2$
Time	$\lambda_T=\sqrt{\lambda_1}=150^{0.5}$		

Table 4 Selection of physical model experimental parameters

Parameters	Length×width/ <i>m</i>	Flow velocity/ cm/s	Rate of flow/ m ³ /s	Ore drawing consistence
Test value	11.0×7.5	8.26	7.9e ⁻³	60%

criterion (Xue *et al.* 2019, Yin *et al.* 2011), the relationship similarity scale of each parameter between the model and the prototype was speculated, as displayed in Table 3.

Froude criterion is the foundation to design the model experiment, which is applicable for the water flow movement similarity criterion when gravity serves as the main acting force (Xue *et al.* 2019, Penel 1975), as expressed below.

$$Fr = \sqrt{\frac{F_I}{F_G}} = \sqrt{\frac{\rho l^2 v^2}{\rho l^3 g}} = \frac{v}{\sqrt{gl}} \quad (1)$$

where Fr represents the Froude number, F_I is the inertial force, F_G is the gravity; v is the velocity, ρ is the density, l is the characteristic length, while g indicates the gravitational acceleration.

The dynamic similarity satisfied the Froude criterion (Penel 1975), namely:

$$Fr_p = Fr_m \quad (2)$$

where Fr_p and Fr_m indicate the Froude numbers of prototype and physical model, respectively.

According to our previous research (Wang *et al.* 2019,

Tian and Chen 2015, Li *et al.* 2020), the tailings flowing process can be deemed as the movement under the combined action of gravity and viscous force, and it is dominated by gravity. Therefore, gravity similarity was selected as the material selection principle, and the Froude criterion should be satisfied when carrying out model experiment.

2.4 Physical model parameters

Model fluid should satisfy the gravity (Froude) similarity criterion and viscous force similarity criterion. Consequently, the mud-rock flow proportion in the test material used in that model was 60%, and tailings from the miner ($d_{50} = 0.034$ mm) were selected as the flowing material in this model experiment. Additionally, Table 4 shows the selection of main physical model experimental parameters.

The tailings impoundment dam model is constituted by four parts, including thoughts, ore drawing system, groundwater level measuring system and the infiltration system. The groundwater level measuring tube was the $\Phi 50$ PPR pipe, which was connected to the $\Phi 5$ lucite pipe to facilitate measurement. The tailings pulp delivery pipe was the $\Phi 75$ PPR pipe, and a spherical valve was placed at the front of the ore drawing branch to control the tailings pulp flow rate. The prepared tailings pulp was stirred using the blender, discharged to the reservoir area via the delivery pipe; in this way, the tailings impoundment accumulation process was simulated. Meanwhile, the changes in water level were read and recorded, and the tailings were sampled on the dry beach surface. Fig. 3 displays the dry beach surface formed during the damming process and the physical model after damming.

3. Result and discussions

3.1 Tailings discharge and damming process

Tailings impoundment is formed due to the deposition of water power ore drawing in dressing mill, and its internal



(a) Groundwater level measuring system and infiltration system (b) Sampling on the dry beach surface of the damming model system

Fig. 4 Groundwater level measuring and sampling method



(a) Tailings pulp fan-shaped diffusion (b) Groove channel on the deposited beach surface

Fig. 5 The tailings deposition pattern of the physical model

structures, such as particle size and pore distribution rules, are the important factors affecting the tailings impoundment stability (Hübl and Steinwendtner 2001, Wei *et al.* 2019). Therefore, it is of great significance to investigate the tailings deposition rules. Fig. 4(a) shows the groundwater level measuring system and the infiltration system of the damming model. While during the damming experimental process, tailings were sampled along the central axis of the model at an interval of 40 cm when piled up to different heights; in addition, every four levels of the fill dam (20 cm) were treated as one layer for sampling, as shown in Fig. 4(b), and the selected tailings samples were performed particle size analysis.

After tailings pulp was discharged from the ore drawing branch, the energy dissipation pit was formed on the deposited beach. This was mainly because that, this tailings pond adopted the multi-tributary disperse ore drawing in front of the dam, so the tailings pulp flowing out from the discharge pipe formed the impact energy dissipation pit around the discharge outlet as a result of pulp impact. And the pulp diffused into the reservoir in a sector manner with the energy dissipation pit as the starting point, due to the dam body obstruction, as shown in Fig. 5(a).

During the tailings pulp diffusion process, the horizontal

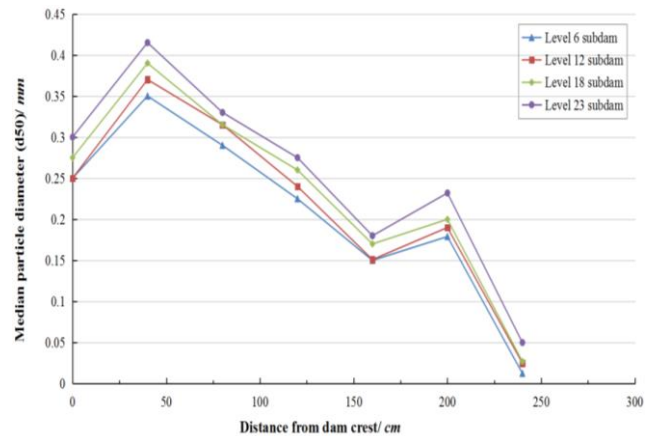


Fig. 6 Changes in median particle diameter (d50) with the distance from the dam crest

flow velocities offset each other at the junction of two sector areas, the flow velocities towards the reservoir superposed each other to increase the flow velocity, which enhanced the capacity to carry sediments. Consequently, the tortuous groove channel was formed on the deposited beach surface, as displayed in Fig. 5(b).

Then, the tailings pulp flowed to the periphery of energy

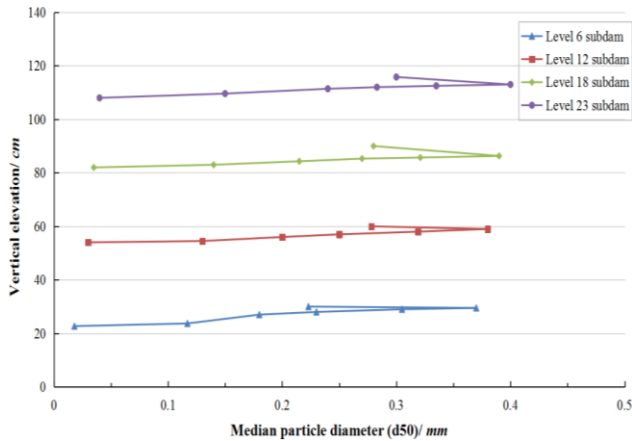


Fig. 7 The relation between the median particle diameter (d_{50}) of dry beach samples and the vertical elevation of deposited beach

dissipation pit and formed the fan-shaped alluvial flat centered on the energy dissipation pit, which was carried by the pulp and flowed to the reservoir tail. In the meantime, most suspended particles with small particle size slowly deposited only in the lentic environment, which might resulted in the obvious reservoir tail refinement phenomenon.

3.2 Tailings deposition characteristics

Fig. 6 exhibits the changes in median particle diameter (d_{50}) with location obtained based on the experimental data. As observed from Fig. 6, the coarse particles were deposited in front of the dam, and the fine particles were distributed around the reservoir tail. With the increase in distance from the dam crest, the median particle diameter (d_{50}) of tailings decreased on the whole. At the junction between the deposited beach that was 200 cm away from the dam crest and the water surface, the median particle diameter increased suddenly. After analysis, this phenomenon might be that, the large particles in tailings pulp were slightly affected by current scour at a place far away from the dam crest, and they continued to move depending on inertia and their own gravity (Kim *et al.* 2019, Okuda *et al.* 1980). During the movement process, their velocity gradually decreased due to the friction of the deposited beach, they stopped moving when they moved to the water surface junction as a result of water obstruction in the reservoir, and finally deposited at the junction between the deposited beach and the water surface.

Fig. 7 shows the relation of median particle diameter with the vertical elevation. As observed from the figure, when the fill dam accumulated upward at a certain slope ratio, the vertical direction of the deposited beach showed periodical changes, which generally manifested as the gradually decreased particle size with the increase in height. Moreover, it was also discovered that, the crest particle size suddenly decreased in each period. This was because that, the sand flow velocity reduced suddenly on the dry beach surface when the discharge stopped, the tailings developed hydrostatic deposition on the deposited beach, thus giving

rise to the phenomenon of first increase and then decrease within each period (Alexey 2016, Mahdi *et al.* 2020).

3.3 Saturation line variation rules

Accurately obtaining the saturation line position in the tailings dam body is the foundation of static and kinetic stability analysis of the dam body. To this end, a device for observing the saturation line was set in the experimental system. When the tailings dam was constructed to various heights, water was injected into the reservoir, and the dry beach length was controlled at 67 cm (equivalent to 100 m in field) and 200 cm (equivalent to 300 m in field), respectively. In addition, the changes in saturation line under flood and normal working conditions were simulated, respectively, and corresponding data were obtained through measuring the water level height of the observation tube, as shown in Fig. 8 and Fig. 9.

As acquired from Figs. 8 and 9, the saturation line gradually elevated with the increase in dam height. Under normal condition, the saturation line buried depth ranged from 4.0 to 88.0 cm at different dam heights, while that under flood condition was 4.0-92 cm. The saturation

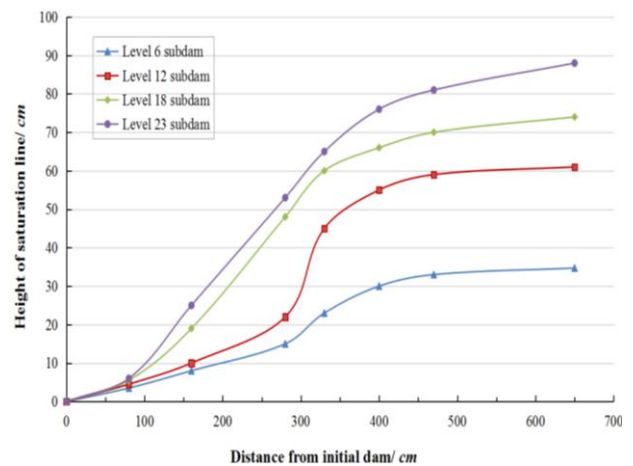


Fig. 8 The saturation lines variation of physical model under normal condition

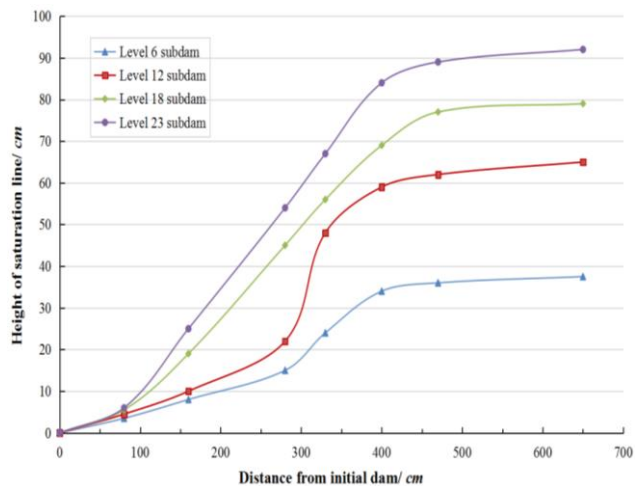


Fig. 9 The saturation lines variation of physical model under flood condition

line variation trend under flood condition was similar to that under normal condition, but the height of saturation line under flood condition was higher than that under normal condition, with the maximum height difference of 4 cm. The saturation line was not markedly changed within the range of 0-1.0 m away from the initial dam, while that was obviously changed with dam height elevation within the range of 1.0-4.5 m away from the initial dam.

Thus, it was clear that, the overall stability of tailings pond declined under the flood working condition, which increased the risk of dam failure. At the same time, the dry beach length of tailings impoundment had great influence on the flood regulation storage capacity. Typically, a longer dry beach length resulted in a greater flood regulation storage capacity and the relatively higher safety. Such experimental conclusion conformed to the engineering practice.

4. Conclusions

With reference to the prototype tailings impoundment design data, this study conducts the tailings laboratory damming model experiments based on the similarity theory for physical simulation of the tailings damming process. Besides, the deposition characteristics of tailings on the dry beach surface during the damming process and the variation rules of dam saturation line are investigated.

- According to our research, the tailings particles gradually become finer along the beach surface axis towards the reservoir, but they suddenly change at the junction between the deposited beach and the water surface, and obvious coarsening phenomenon can be observed. As the fill dam is accumulated upward at a certain slope ratio, the deposited beach shows the vertical feature of coarse upward and fine downward, and the crest particle diameter suddenly decreases in each period.

- Moreover, phenomena such as alternating changes of particle size, and thick and thin interlayer, are observed at different depths

- In the meantime, the saturation line gradually elevates as the dam height increases; the dam saturation line is not markedly changed within the range of 0-1.0 m away from the initial dam, while that is obviously changed with dam height elevation within the range of 1.0-4.5 m away from the initial dam (in the model)

- The variation trend of saturation line under flood condition is similar to that under normal condition, but the height of saturation line under flood condition is higher than that under normal condition, with the maximum height difference of 4 cm.

This paper applies the related soil mechanical tests and laboratory model experiments in investigation, and the research results can provide theoretical foundation for tailings dam stability analysis, as well as dam break-induced disaster prevention and mitigation.

Author contributions

Guangjin Wang: Methodology, Software, Data curation,

Formal analysis, Visualization, Writing-Original draft preparation. Sen Tian: Conceptualization, Investigation, Data curation, Formal analysis, Funding acquisition, Supervision, Project administration, Writing-Original draft preparation, Writing-Reviewing and Editing. Bin Hu, Jie Chen and Xiangyun Kong: Methodology, Validation, Writing-Original draft preparation. All authors gave final approval for publication.

Acknowledgments

The research described in this paper was financially supported by the National key research and development plan [grant number 2017YFC0804600]; the National Natural Science Foundation of China [grant numbers U1802243; 51904040; 41672317]; the Fundamental Research Funds for the Central Universities [grant number 2020CDJQY-A045; 2020CDJ-LHZZ-003]; the Open issue with “the key laboratory of mine geological hazards mechanism and Hubei province technical innovation special (Major projects)” [grant number 2017ACA184]; the General Program of Chongqing Natural Science Foundation Project [grant number cstc2020jcyj-msxmX0747]; and the Program for Changjiang Scholars and Innovative Research Team in University [grant number IRT_17R112].

The authors would like to acknowledge the colleagues from the State Key Laboratory of Coal Mine Disaster Dynamics and Control for their perspectives and suggestions related to data collection and statistical analysis.

References

- Alexey, K. (2016), “Modeling and observations of geyser activity in relation to catastrophic landslides-mudflows (Kronotsky nature reserve, Kamchatka, Russia)”, *J. Volcanol. Geoth. Res.*, **323**, 129-147. <https://doi.org/10.1016/j.jvolgeores.2016.05.008>.
- Alhasan, Z., Jandora, J. and Riha, J. (2016), “Comparison of specific sediment transport rates obtained from empirical formulae and dam breaching experiments”, *Environ. Fluid Mech.*, **16**(5), 1-23. <https://doi.org/10.1007/s10652-016-9463-2>.
- Aly, A., Keizo, U. and Yang, Q. (2012), “Assessment of 3D Slope Stability Analysis Methods Based on 3D Simplified Janbu and Hovland Methods”, *Int. J. Geomech.*, **12**(2), 81-89. [https://doi.org/10.1061/\(ASCE\)GM.1943-5622.0000117](https://doi.org/10.1061/(ASCE)GM.1943-5622.0000117).
- Cai, S., Tang, Q., Tian, S., Lu, Y. and Gao, X. (2019), “Molecular simulation study on the microscopic structure and mechanical property of defect-containing sl methane hydrate”, *Int. J. Mol. Sci.*, **20**(9), 2305. <https://doi.org/10.3390/ijms20092305>.
- Darren, L., Caitlin, M., Craig, G., Roca, C.M., Gregor, P. and Mark, W. (2019), “The potential to reduce the risks posed by tailings dams using satellite-based information”, *Int. J. Disast. Risk Re.*, **38**. <https://doi.org/10.1016/j.ijdr.2019.101209>.
- Deng, D., Li, L., Wang, J. and Zhao, L. (2016), “Limit equilibrium method for rock slope stability analysis by using the Generalized Hoek-Brown criterion”, *Int. J. Rock Mech. Min. Sci.*, **89**, 176-184. <https://doi.org/10.1016/j.ijrmms.2016.09.007>.
- Dutto, P., Stickle, M.M., Pastor, M., Manzanal, D., Yague, A., Moussavi Tayyebi, S., Lin, C. and Elizalde, M.D. (2017), “Modelling of fluidised geomaterials: The case of the Aberfan

- and the Gypsum tailings impoundment flowslides”, *Materials*, **10**(5), 562. <https://doi.org/10.3390/ma10050562>.
- Gawu, S.K. and Fourie, A.B. (2004), “Assessment of the modified slump test as a measure of the yield stress of high-density thickened tailings”, *Can. Geotech. J.*, **41**(1), 39-47. <https://doi.org/10.1139/T03-071>.
- Hübl, J. and Steinwendtner, H. (2001), “Two-dimensional simulation of two viscous debris flows in Austria”, *Phys. Chem. Earth*, **26**(9), 639-644. [https://doi.org/10.1016/S1464-1917\(01\)00061-7](https://doi.org/10.1016/S1464-1917(01)00061-7).
- Jia, T., Wang, R., Fan, X. and Chai, B. (2018), “A comparative study of fungal community structure, diversity and richness between the soil and the phyllosphere of native grass species in a copper tailings dam in Shanxi Province, China”, *Appl. Sci.*, **8**(8), 1297. <https://doi.org/10.3390/app8081297>.
- Jing, X., Chen, Y., Xie, D., Williams, D.J., Wu, S., Wang, W. and Yin, T. (2019), “The effect of grain size on the hydrodynamics of mudflow surge from a tailings dam-break”, *Appl. Sci.*, **9**(12), 2474. <https://doi.org/10.3390/app9122474>.
- Kim, B.S., Kato, S. and Park, S.W. (2019), “Experimental approach to estimate strength for compacted geomaterials at low confining pressure”, *Geomech. Eng.*, **18**(5), 459-469. <https://doi.org/10.12989/gae.2019.18.5.459>.
- Li, S., Yuan, L., Yang, H., An, H. and Wang, G. (2020), “Tailings dam safety monitoring and early warning based on spatial evolution process of mud-sand flow”, *Safety Sci.*, **124**. <https://doi.org/10.1016/j.ssci.2019.104579>.
- Mahdi, A., Shakibaenia, A. and Dibike, Y.B. (2020), “Numerical modelling of oil-sands tailings dam breach runoff and overland flow”, *Sci. Total Environ.*, **703**, 134568. <https://doi.org/10.1016/j.scitotenv.2019.134568>.
- Marsooli, R. and Wu, W. (2014), “3-D finite-volume model of dam-break flow over uneven beds based on VOF method”, *Adv. Water Resour.*, **70**, 104-117. <https://doi.org/10.1016/j.advwatres.2014.04.020>.
- Mizani, S. (2010), “Rheology of thickened gold tailings for surface deposition”, Master Dissertation, Carleton University, Ottawa, Canada.
- Muceku, Y., Korini, O. and Kuriqi, A. (2016), “Geotechnical analysis of Hill's slopes areas in heritage town of Berati, Albania”, *Period. Polytech. Civ.*, **60**(1), 61-73. <https://doi.org/10.3311/PPci.7752>.
- Nam, D.H., Kim, M.I., Kang, D.H. and Kim, B.S. (2019), “Debris flow damage assessment by considering debris flow direction and direction angle of structure in South Korea”, *Water*, **11**, 328. <https://doi.org/10.3390/w11020328>.
- Okuda, S., Okunishi, K. and Suwa, H. (1980), “Observation of Debris flow at Kamikamihori Valley of Mt. Yakedake”, *Proceedings of the 3rd Meeting of IGU Commission on Field Experiment in Geomorphology*, Kyoto, Japan, August.
- Owen, J.R., Kemp, D., Lèbre, È., Svobodova, K. and Murillo, G.P. (2020), “Catastrophic tailings dam failures and disaster risk disclosure”, *Int. J. Disast. Risk Re.*, **42**, 101361. <https://doi.org/10.1016/j.ijdr.2019.101361>.
- Parbhakar-Fox, A., Glen, J. and Raimondo, B. (2018), “A geometallurgical approach to tailings management: An example from the savage river Fe-Ore mine, Western Tasmania”, *Minerals*, **8**(10), 454. <https://doi.org/10.3390/min8100454>.
- Pashias, N. (1996), “A fifty cent rheometer for yield stress measurement”, *J. Rheol.*, **40**(6), 1179. <https://doi.org/10.1122/1.550780>.
- Penel, J. (1975), “Froude criterion for ice-block stability”, *J. Glaciol.*, **14**(71), 341-342. <https://doi.org/10.3189/S0022143000021870>.
- Rico, M., Benito, G. and Díez-Herrero, A. (2008), “Floods from tailings dam failures”, *J. Hazard. Mater.*, **154**(1-3), 79-87. <https://doi.org/10.3390/w11020328>.
- Santamarina, C.J., Torres-Cruz, L.A. and Bachus, R.C. (2019), “Why coal ash and tailings dam disasters occur”, *Science*, **364**(6440), 526-528. <https://doi.org/10.1126/science.aax1927>.
- Sun, E., Zhang, X. and Li, Z. (2012), “The internet of things (IOT) and cloud computing (CC) based tailings dam monitoring and pre-alarm system in mines”, *Safety Sci.*, **50**(4), 811-815. <https://doi.org/10.1016/j.ssci.2011.08.028>.
- Tian, S., Chen, J. and Dong, L. (2017), “Rock strength interval analysis using theory of testing blind data and interval estimation”, *J. Central South Univ.*, **24**(1), 168-177. <https://doi.org/10.1007/s11771-017-3418-8>.
- Tian, S. and Chen, J. (2015), “Multi-hierarchical fuzzy judgment and nested dominance relation of the rough set theory-based environmental risk evaluation for tailings reservoirs”, *J. Central South Univ.*, **22**(12), 4797-4806. <https://doi.org/10.1007/s11771-015-3031-7>.
- Wang, G., Tian, S., Hu, B., Xu, Z., Chen, J. and Kong, X. (2019), “Evolution pattern of tailings flow from dam failure and the buffering effect of debris blocking dams”, *Water*, **11**(11), 2388. <https://doi.org/10.3390/w11112388>.
- Wang, K., Yang, P., Hudson-Edwards, K.A., Lyu, W., Yang, C. and Jing, X. (2018), “Integration of DSM and SPH to model tailings dam failure run-out slurry routing across 3D real terrain”, *Water*, **10**(8), 1087. <https://doi.org/10.3390/w10081087>.
- Wei, Z., Chen, Y., Yin, G., Yang, Y. and Shu, W. (2019), “An alternative upstream method for the Zhelamuqing tailings impoundment construction of a Copper Mine in China”, *Geomech. Eng.*, **19**(5), 383-392. <https://doi.org/10.12989/gae.2019.19.5.383>.
- Wei, Z., Yin, G., Wang, J., Wan, L. and Li, G. (2013), “Design, construction and management of tailings storage facilities for surface disposal in China: Case studies of failures”, *Waste Manage Res.*, **31**(1), 106-112. <https://doi.org/10.1177/0734242X12462281>.
- Xue, H., Ma, Q., Diao, M. and Jiang, L. (2019), “Propagation characteristics of subaerial landslide-generated impulse waves”, *Environ. Fluid Mech.*, **19**(1), 203-230. <https://doi.org/10.1007/s10652-018-9617-5>.
- Yin, G., Li, G., Wei, Z., Wan, L., Shui, G. and Jing, X. (2011), “Stability analysis of a copper tailings dam via laboratory model tests: A Chinese case study”, *Miner. Eng.*, **24**(2), 122-130. <https://doi.org/10.1016/j.mineng.2010.10.014>.
- Zhang, L., Tian, S. and Peng, T. (2019), “Molecular simulations of sputtering preparation and transformation of surface properties of Au/Cu alloy coatings under different incident energies”, *Metals*, **9**(2), 59. <https://doi.org/10.3390/met9020259>.
- Zheng, B., Zhang, D., Liu, W., Yang, Y. and Yang, H. (2019), “Use of basalt fiber-reinforced tailings for improving the stability of tailings dam”, *Materials*, **12**(8), 1306. <https://doi.org/10.3390/ma12081306>.
- Zhou, X. and Cheng, H. (2014), “Stability analysis of three-dimensional seismic landslides using the rigorous limit equilibrium method”, *Eng. Geol.*, **174**, 87-102. <https://doi.org/10.1016/j.enggeo.2014.03.009>.